Improved Test Methods for Polymer Additive Manufacturing Interlayer Weld Strength and Filament Mechanical Properties

Richard G. Cole,[1] Kazem Fayazbakhsh,[2] Abraham Avalos,[3] and Nicholas A. Nadeau[4]

[1]National Research Council Canada, Aerospace Research Centre, Ottawa, K1A 0R6, Canada

https://orcid.org/0000-0003-0453-5048

[2]Aerospace Engineering Department, Ryerson University, Toronto, M5B 2K3, Canada,

https://orcid.org/0000-0003-3963-8282

[3]AON3D, Montreal, H2N 1P4, Canada A. A. https://orcid.org/00 00-0001-6980-4734, N. A. N.

https://orcid.org/0000-0003-1220-0889

STP 1637, 2022 / available online at www.astm.org

https://doi.org/10.1520/STP163720200107

ABSTRACT

The international community is exploring many potential end uses for polymer additive manufacturing. However, significant issues must be addressed before broad application can occur, in particular understanding the relationships between materials, processes, and final part properties. Key to these issues is having reliable test methods to measure properties of interest. This work used an AON-M2 industrial printer to investigate material extrusion manufacturing. Past research has frequently shown interlayer weld strength (i.e., *Z*-direction strength) is the weakest property in material extrusion parts and has also shown this property is difficult to measure, with significant data scatter and poor failure modes common for tensile specimens printed vertically. Using acrylonitrile butadiene styrene, the current work investigated in-plane shear testing to interrogate interlayer weld strength based on ASTM D3846, *Standard Test Method for In-Plane Shear Strength of Reinforced Plastics*, which uses a notched coupon loaded in compression. Further, a modified version of ASTM D3846 was investigated using smaller unnotched "minishear coupons." Both test methods were found to provide very consistent results, with coefficients of variation of 5% or less; however, the ASTM D3846 notched coupons showed evidence of excessive gage section rotation and interference with the test fixture. The minishear test method did not have this problem and also allowed direct measurement of strain, thereby providing shear modulus. The authors note that in assessing the effect of process on properties, choice of the basis of comparison is important. While many researchers use injection molded properties, the authors believe this is misleading because the injection molding process itself affects properties. Instead, the authors investigated measurement of the polymer filament directly. New methods for filament shear and tension testing were developed that provided good coefficients of variation and allowed direct comparison between three-dimensional printed coupon

properties and filament properties in shear.

Keywords

additive manufacturing, material extrusion, MEX, fused filament fabrication, interlayer, weld, shear, filament properties, ABS

Introduction

The material extrusion (MEX) process (also known as fused filament fabrication or FFF) is a popular three-dimensional (3D) printing technique that allows manufacturing of parts from a wide range of materials including polymers. In this process, a filament is continuously fed into an extrusion nozzle, is heated to a molten state, and is deposited onto a build platform. In general, material is deposited in the *X*-*Y* plane to create each layer followed by offsets in the nozzle or build platform in the *Z* direction to allow placement of subsequent layers.

To explore the effect of the MEX process on properties, many researchers have used ASTM D638, *Standard Test Method for Tensile Properties of Plastics*, Type I tensile specimens[1,2] and have generally found that the upright build orientation (*ZXY/ZYX*) results in significantly lower properties than the flat (*XYZ/YXZ*) and on-edge build orientations (*XZY/YZX*), which has led to general recognition of the need to improve interlayer weld strength.[3–6] But it has also been found that these upright tensile results often exhibit high variability and frequent failures in the transition area of the specimens,[7] indicating this is a difficult and unreliable test for interrogating the interlayer weld. To avoid these problems, the authors decided to measure interlayer weld properties through in-plane shear loading. ASTM D3846, *Standard Test Method for In-Plane Shear Strength of Reinforced Plastics*,[8] was selected as the basis for this work, with a notched coupon loaded in compression to measure in-plane shear properties. An improvement to this method using "minishear coupons" was also investigated.

To accurately assess the effect of the MEX process on final part properties, the authors recognized the importance of determining a suitable basis for the baseline or "bulk material" properties for comparison. Many researchers have used injection molded properties, but this can be misleading because the injection molding process affects properties. Instead, the authors proposed considering the incoming material to the MEX process, the polymer filament, as the basis for comparison. Because there is a lack of standardized tests for filaments, many researchers have struggled to obtain reliable measurements,[3,9,10] and the authors undertook to develop suitable methods for measuring filament shear and tensile properties. A test using sliding plates in double shear was investigated, and for tensile testing, a novel grip was designed and 3D printed to minimize stress concentrations on the filament. While the intention of this work was to provide data on bulk properties for comparison to 3D printed coupon properties, it is recognized that they may also be useful for filament quality assurance purposes.

The material chosen for this work was acrylonitrile butadiene styrene (ABS) Prime from AON3D (Montreal, Canada). To minimize the effects of material batch-to-batch variability, AON3D was able to supply material from a single batch, on three sequentially numbered spools, one to each partner. To include the effects of manufacturing variability in this work, wherever possible efforts were made to test specimens from three manufacturing batches.

Measuring Interlayer Weld Strength

Efforts to measure interlayer weld properties began with the ASTM D3846 test method, which uses a notched coupon loaded in compression to measure in-plane shear properties. Previous tests with polyetheretherketone (PEEK) specimens found a 0.25-in. (6.4 mm) thick coupon, notched through to the midplane from each side in order to apply interlayer shear load in the *XY* plane, gave good results.[11] While this approach with notched coupons was used in the current work, an alternate approach using minishear coupons was also developed. In this second method, cuts were made fully through the thickness to create short coupons of the same length as the gage section in the notched coupons, and steel plates were used to apply in-plane shear loads. Details are given in the following paragraphs.

COUPON MANUFACTURE

The interlayer weld strength specimens were manufactured by AON3D as rectangular blocks with a nominal thickness of 0.25 in. (6.40 mm), a width of 0.50 in. (12.7 mm), and a length of 3.21 in. (81.5 mm). The blocks were all printed flat on the build plate in the *YXZ* orientation defined in ISO/ASTM 52921, *Standard Terminology for Additive Manufacturing—Coordinate Systems and Test Methodologies*,[12] with all beads aligned in the lengthwise direction except for a short turnaround area at each end. The G-code was generated using Simplify3D slicer software, version 4.1.2, and no shrinkage compensation. Process conditions were carefully optimized (values from G-code):

- Layer height: 0.008 in. (0.2mm).
- Bead width: 0.032 in. (0.82mm).
- Printing speed: 1.8 in./s (45mm/s).
- Perimeter number of outlines: 10 (direction outside in).
- Chamber temperature: 194°F (90°C).
- Bed temperature: 212°F (100°C).
- Extrusion temperature: 455°F (235°C).

- Extrusion multiplier: 1.00.
- Infill percentage: 100 (single extrusion).
- First layer (only) printed at 50% of nominal speed and 473°F (245°C).

Before printing, the AON3D ABS Prime filament was dried at 140°F (60°C) for 4 hours in an air recirculating oven then, during printing, the spool was kept inside a room-temperature dry box with humidity between 4% and 7%. Between the dry box and the printer, the filament path was protected by polytetrafluoroethylene (PTFE) tubing. The coupon blocks were printed in three batches of ten, layer by layer, in the same locations, by a single AON-M2 industrial printer equipped with a Kapton-aluminum bed and a tool head with a Copper Volcano block hot-end (E3D, UK) and a PT100 RTD Temperature Sensor (Dyze, Canada). A 0.025 in. (0.6 mm) diameter hardened steel Volcano nozzle (E3D, UK) was used. Blocks were printed directly on the Kapton surface (i.e., no raft). After printing, blocks were left to cool to approximately 120°F (50°C) before being removed. Microscopic cross-section analysis found minimum voids between beads, even following careful polishing (fig. 1). This suggests the process was very highly optimized and blocks were as solid as is possible with MEX printing, providing a significant challenge for interlayer weld testing.

FIG. 1 ABS prime coupon block cross section.

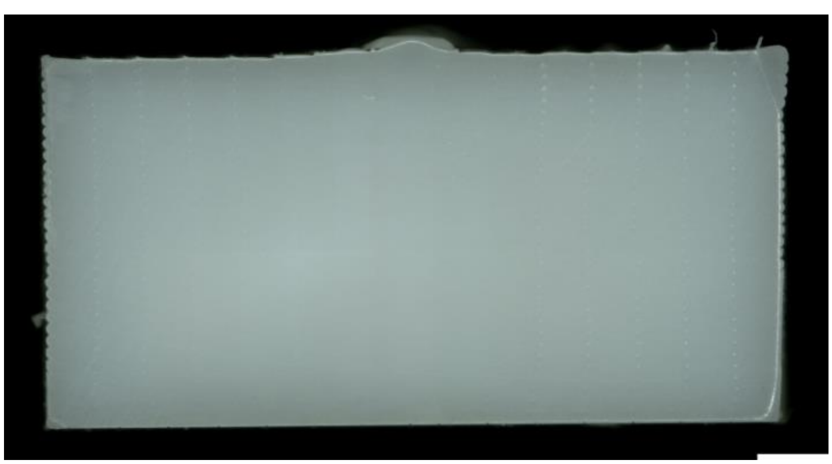

Coupon blocks were prepared for machining using precision sanding to create smooth, flat datums on the bottom and top surfaces and on one edge. Specimens for the ASTM D3846 notched coupon test were prepared using a purpose-built fixture and a wet diamond saw to accurately trim the ends and cut notches through to the coupon midplane within 0.002 in. (0.05 mm). Preparation of minishear coupons used a different fixture to cut nominal lengths of 0.25 in. (6.4 mm), to extract seven minishear coupons from each coupon block. Following machining, all coupons were inspected using a stereomicroscope to verify no defects.

INTERLAYER SHEAR TESTING

The notched coupon tests were performed in accordance with ASTM D3846, which uses the ASTM D695, *Standard Test Method for Compressive Properties of Rigid Plastics*, fixture that uses plates, each with four ridges, to support the specimen. Figure 2 shows the coupon and fixture as well as a coupon pre- and posttest. This test provided measurement of load versus test-frame actuator displacement.

FIG. 2 Notched coupon test method: (*A*) coupon; (*B*) fixture; (*C*) ready to test; and (*D*) posttest.

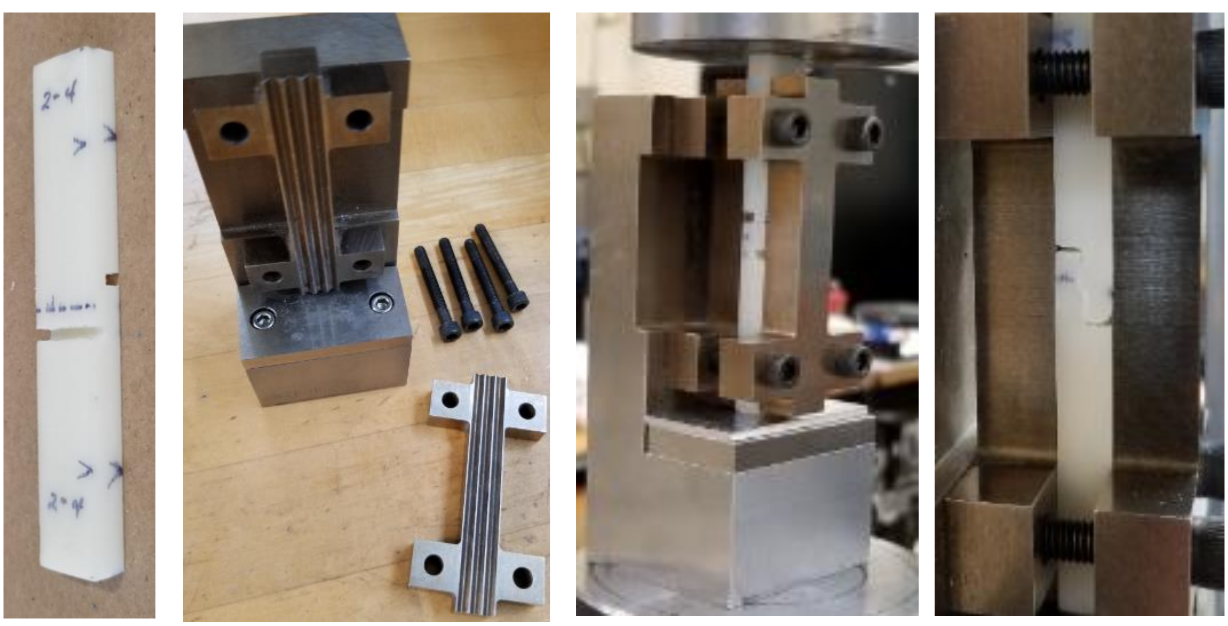

(A) (B) (C) (D)

The minishear coupon test was developed as an improvement to the notched coupon method, using a small coupon of the same length as the gage section of the notched coupon and sliding steel plates to apply shear loads in the ASTM D695 fixture. Plate thicknesses were chosen to provide clearance so the plates could slide freely. This method permitted many small coupons to be taken from each coupon block and allowed a direct measurement of the coupon deformation via an extensometer mounted on the plate edges. Figure 3 shows the sliding steel plates, the assembly in the fixture with a minishear coupon, the extensometer, and a coupon posttest. This test method provides not only measurement of load and actuator displacement, but the extensometer provides accurate measurement of coupon deformation, which allows determination of strain and, therefore, shear modulus. For both test methods, the test rate was selected to be "quasistatic" at 0.05 in./min. (1.3 mm/min.).

FIG. 3 Minishear coupon test method: (*A*) sliding steel plates; (*B*) coupon and plates assembled into fixture; (*C*) extensometer; and (*D*) posttest.

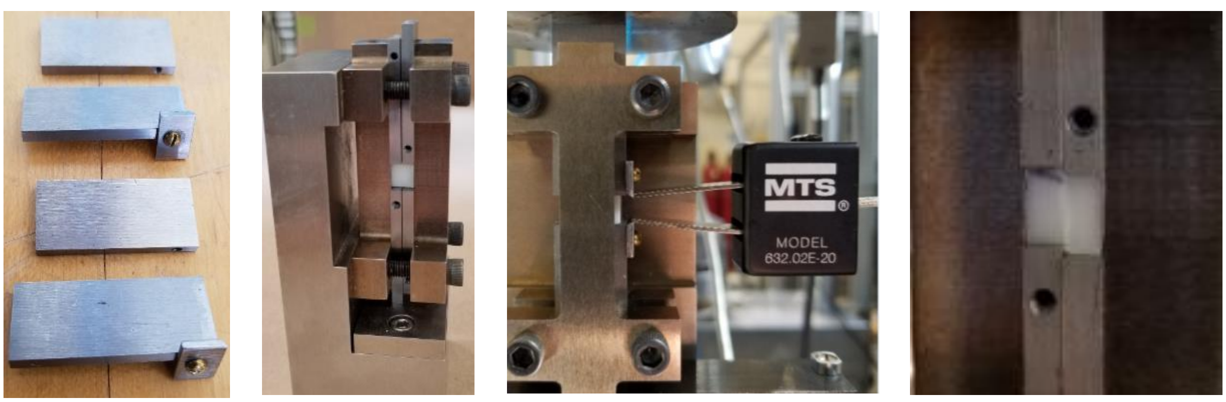

(A) (B) (C) (D)

INTERLAYER SHEAR RESULTS

Typical graphs from notched coupon and minishear coupon tests are shown in figure 4. (Note: The notched coupon *X*-axis is test-frame actuator displacement.) For the minishear coupons, shear modulus was determined over the initial linear portion between 100 and 300 lbf (445 and 1330 N) load. Three batches of coupons were tested using each method, followed by inspection using a stereomicroscope.

FIG. 4 Typical coupon shear test graphs: (*A*) notched coupon and (*B*) minishear coupon.

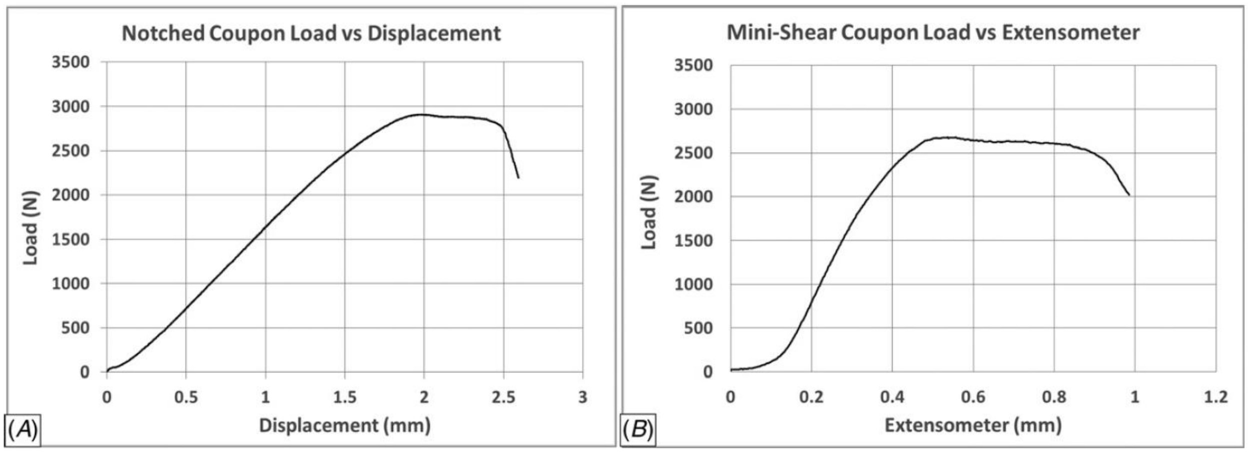

From posttest inspection, all notched coupons showed four to six layers were engaged in the shear failure, and it was clear that a significant amount of detrimental gage section rotation had occurred. Figure 5 shows the evidence, where the broken coupon half shows permanent deformation in the remaining gage section half (a white line is drawn parallel to the coupon main body) and the outside surface of the coupon under the notch region shows significant indentations from the test fixture support ridges. All minishear coupons showed two layers were involved in the shear failure, and there was no evidence of significant rotation.

FIG. 5 Notched coupon and minishear coupon post-test: (*A*) notched coupon—side; (*B*) notched coupon—surface; and (*C*) minishear coupon—side.

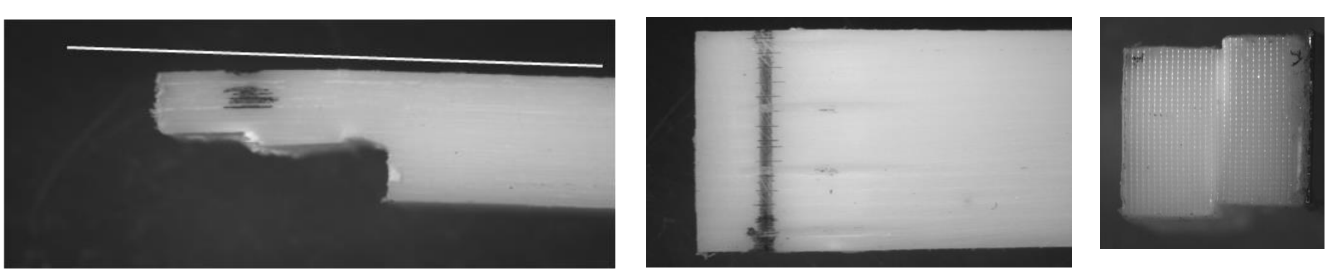

(A) (B) (C)

The interlayer weld properties determined from these tests are summarized in table 1, with all values being from five to seven replicates. For both coupon types, shear strength values were very repeatable with low coefficients of variation (CV = standard deviation/average) within and across batches. The notched coupon strength was found to be more than 9% higher than the minishear coupon strength, and this is believed to have been caused by gage section rotation and interference with the test fixture. For the minishear coupons, shear modulus values showed good repeatability with moderate CVs within and across batches. From both strength and modulus values, batch-to-batch variability was found to be low.

TABLE 1 Interlayer weld shear test results

	NOTCHED COUPON				**MINISHEAR COUPON**			
	Shear Strength		**Shear Modulus**		**Shear Strength**		**Shear Modulus**	
	AVG, psi (MPa)	CV (%)	AVG	CV	AVG, psi (MPa)	CV (%)	AVG, psi (MPa)	CV (%)
Batch 1	5,504 (37.95)	2.9	NA		4,938 (34.04)	2.8	104,178 (718.28)	5.2
Batch 2	5,382 (37.11)	2.5	NA		4,968 (34.26)	1.3	116,205 (801.20)	3.2
Batch 3	5,464 (37.67)	3.2	NA		5,076 (34.99)	1.7	115,427 (795.84)	8.2
OVERALL	**5,447 (37.55)**	**2.9**	**NA**		**4,989** (34.40)	**2.2**	**111,731** (770.36)	**7.4**

Measuring Filament Properties

With a desire to use filament properties as a basis for bulk material properties, the authors recognized not only that new methods were needed to measure the filament mechanical properties of interest but also that the extrusion process used during creation of the filament might affect its properties. In his work on ABS, Rodriguez[13] suggested, “The mechanical properties of thermoplastic polymer materials are significantly affected by the degree of molecular orientation …” caused by the filament manufacturing process. In order to minimize this effect and allow the polymer molecules to take a more random orientation, he suggested oven-treating filament several hours at a temperature above the material's glass transition temperature (T_g), with shrinkage in filament length indicating the extent of internal molecular reorientation. The authors considered this important to determining an accurate basis for comparison because melting of the filament inside the MEX hot end should result in completely random orientation of molecules at that point in the process, regardless of how different printing parameters affect final part properties.

Differential scanning calorimetry tests of ABS Prime at a rate of 18°F (10°C) per minute found the material's T_g to be 212°F (100°C), so oven treatments of 6 h in air at 230°F (110°C) were applied to filament samples (the same cycle as used by Rodriguez). Measurements after treatment found filament diameter had increased by 9% while length had reduced by 17%. Therefore, both untreated and oven-treated samples were tested for the properties of interest.

FILAMENT SHEAR TESTING AND RESULTS

For comparison to interlayer weld shear strength, a filament shear test was developed based on ASTM B565, *Standard Test Method for Shear Testing of Aluminum and Aluminum-Alloy Rivets and Cold-Heading Wire and Rods*,[14] (which is intended for testing aluminum wire). The resulting fixture and test are shown in figure 6. This fixture used 0.25-in. (6.4mm) steel plates to apply double shear to the sample while allowing the use of extensometers. Initially, after measuring the diameters of a large number of filaments, a 0.0720-in. (1.83 mm) hole was reamed through the fixture, but following oven-treatment of the ABS Prime filament, a second 0.0760-in. (1.93 mm) hole was added.

FIG. 6 Filament shear test method: (*A*) fixture side view; (*B*) fixture overall view; and (*C*) fixture with extensometers ready to test.

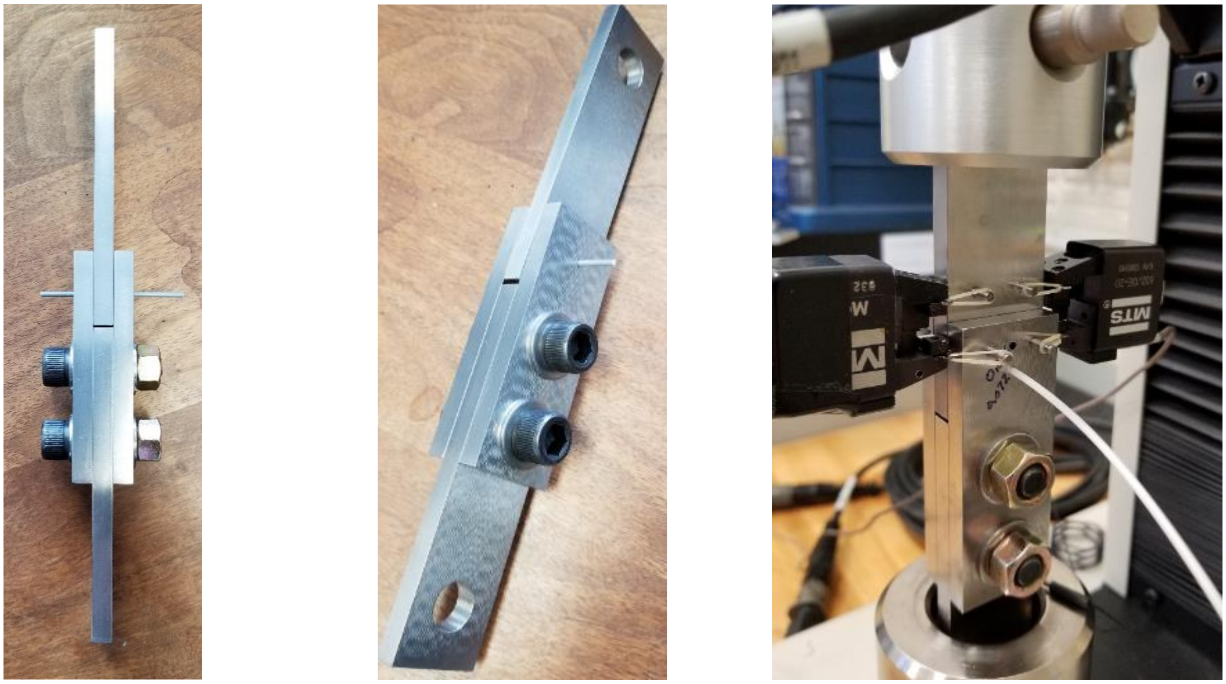

(A) (B) (C)

The inclusion of extensometers provided accurate measurement of filament deformation. For shear strain and, therefore, modulus to be determined, a reference length was needed that was independent of filament geometry (e.g., testing an oval filament in the short versus the long direction should not change total shear strain). Based on the "unit cell" approach, it was decided to use a reference length derived from a square with the same area as the cross section of the filament. The test rate was selected to be quasistatic at 0.05 in./min. (1.3 mm/min.). While all samples used in this work were from the same material batch, the intent of including manufacturing batch effects in the test data was fulfilled by treating filament samples in three separate oven treatments.

The graph from a typical filament shear test is given in figure 7. It shows an initial linear response followed by a peak marked as "Initial Failure," followed by a second extended peak indicating a further increase in load over a much larger displacement. It is believed the second peak is caused by the high ductility of ABS causing incomplete failure of the cross section, with the further increased load caused by filament/fixture interaction. Therefore, all shear strength results shown herein are based on the initial failure peak. Shear modulus was determined over the initial linear portion of the curve, from approximately 10 to 25 lbf load (9 to 23 MPa stress).

FIG. 7 Typical filament shear test graph.

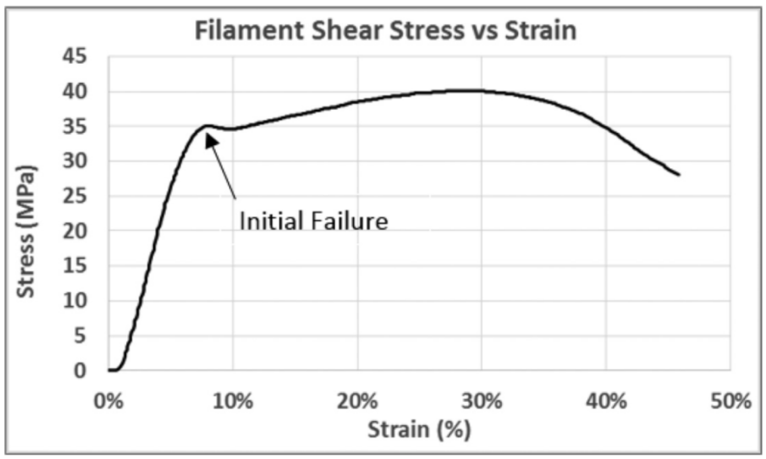

The strength and modulus results from three batches of untreated and oven-treated filaments are shown in table 2. All data points are based on five to seven replicates. It can be seen that for both filament types, shear strength was very repeatable, with very low CVs, and shear modulus had reasonable repeatability (moderate CVs), both within batches and across batches. Overall, the oven-treated filament showed a 4.3% reduction in strength and a 9.0% increase in modulus compared to the untreated filament. The increase in shear modulus supports the idea of oven treatment reducing the preferential alignment of ABS molecules in the filament extrusion direction because a more random orientation should provide higher initial transverse shear stiffness.

TABLE 2 Filament shear test results

	UNTREATED FILAMENT				OVEN-TREATED FILAMENT			
	Shear Strength		Shear Modulus		Shear Strength		Shear Modulus	
	AVG, psi (MPa)	CV (%)	AVG, psi (MPa)	CV (%)	AVG, psi (MPa)	CV (%)	AVG, psi (MPa)	CV (%)
Batch 1	5,072 (34.97)	0.5	98,057 (676.08)	4.7	4,752 (32.76)	1.0	102,376 (705.86)	6.1
Batch 2	5,059 (34.88)	0.6	95,149 (656.03)	6.6	4,815 (33.20)	1.2	102,639 (707.67)	6.3
Batch 3	4,985 (34.37)	0.8	92,625 (638.63)	10.4	4,900 (33.78)	1.6	107,165 (738.88)	6.9
OVERALL	**5,038 (34.74)**	**1.0**	**95,451 (658.11)**	**7.2**	**4,822 (33.25)**	**1.9**	**104,060 (717.47)**	**6.4**

FILAMENT TENSILE TESTING AND RESULTS

Some of the authors' previous work had shown it was difficult to introduce tensile load into a filament specimen without a stress concentration,[10] so a novel grip was designed and 3D printed from polylactic acid (PLA). The minimum spooling radii of various filaments and head displacement limits of the testing machine were considered, and a 3.15-in. (80 mm) diameter was selected. A clamping system using nuts and screws was used to fix the filament's free end. The stiffness of the grip was increased by the addition of a crossbar in the design, and the grip was proven to only deform 0.02 in. (0.5 mm) under 200 lbf (890 N) load (fig. 8).

FIG. 8 Filament tensile test method.

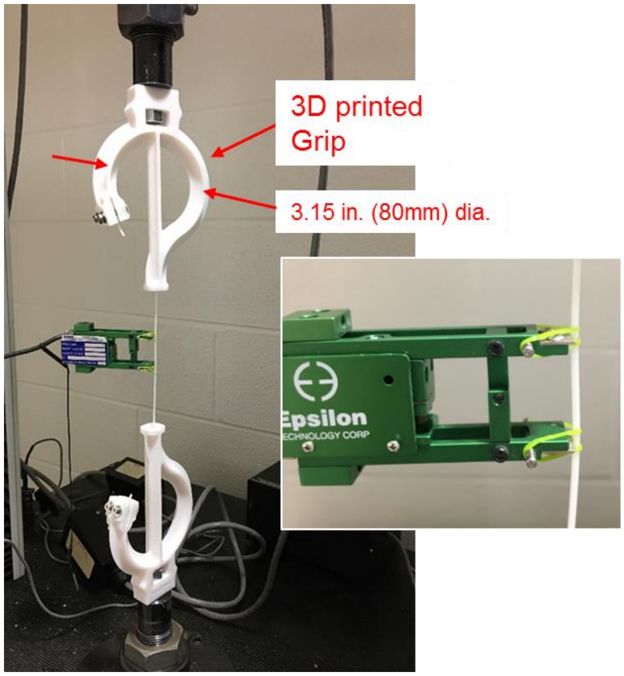

An extensometer with a 25% elongation limit was attached to the filament using two elastic bands to measure strain. A constant head displacement rate of 0.2 in./min. (5 mm/min.) was used; load and strain were measured to failure. Figure 9 shows a stress-strain graph for representative untreated and oven-treated filaments.

FIG. 9 Typical stress-strain graphs from filament tensile tests.

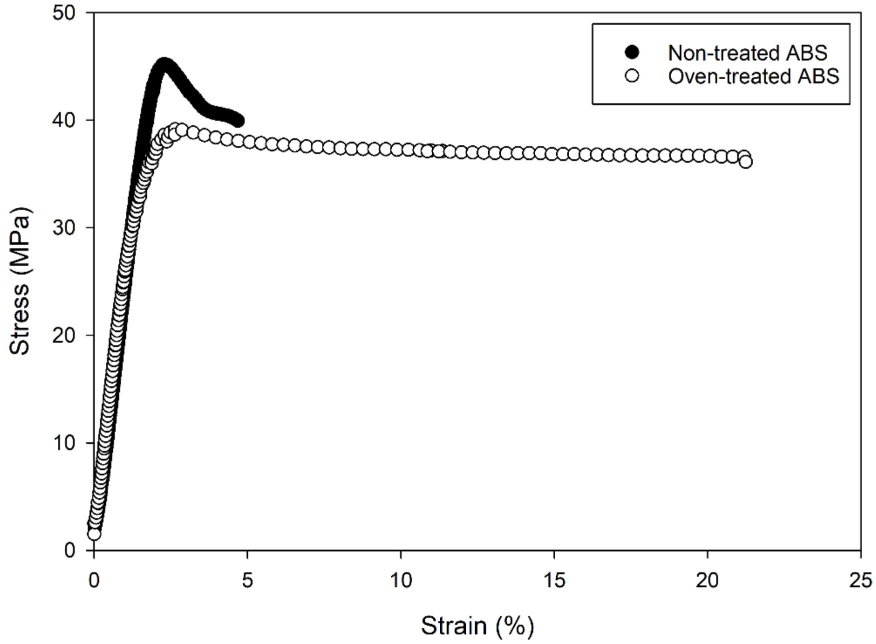

Table 3 summarizes the results. For untreated filament, tensile strength includes 13 data points, while Young's modulus and failure strain include eight and five data points, respectively. For oven-treated filament, seven data points were evaluated for all properties.

TABLE 3 Filament tensile test results

	Tensile Strength		Young's Modulus		Failure Strain	
Sample	AVG, psi (MPa)	CV (%)	AVG, ksi (GPa)	CV (%)	AVG (%)	CV (%)
Untreated ABS	6,529 (45.0)	1.2	357.9 (2.47)	8.3	4.51	14.2
Oven-Treated ABS	5,712 (39.4)	0.7	349.1 (2.41)	9.2	> 20	N/A

The oven-treated filament showed reductions of 12% in strength and 2.5% in modulus compared to untreated filament. This further supports the idea that oven treatment reduces preferential alignment of polymer molecules in the filament extrusion direction. Specimen failure always occurred within the gauge section (i.e., between the grips), which shows the robustness of the test technique. The concerns identified during testing were as follows: extensometer attachment using elastic bands was not robust, and strain measurement at failure was not accurate when specimen necking happened outside the extensometer grip. Future work will address these concerns.

Shear Properties Comparison

Comparing shear results from all tests (table 4), interlayer weld shear strength as determined by the minishear coupons was very similar to the bulk shear strength as represented by the filament tests. Meanwhile, at these high interlayer weld strengths, the notched coupons suffered from excessive gage section rotation, which caused interference with the test fixture and suspect shear strength values. The interlayer weld shear modulus was determined to be 7.4% higher than the bulk property represented by the oven-treated filament; however, the results were within one standard deviation.

TABLE 4 Comparison of filament and interlayer shear test results

	Shear Strength		**Shear Modulus**	
	AVG, psi (MPa)	CV (%)	AVG, psi (MPa)	CV (%)
Untreated Filament	5,038 (34.74)	1.0	95,451 (658.11)	7.2
Oven-Treated Filament	4,822 (33.25)	1.9	104,060 (717.47)	6.4
Notched Coupon	5,447 (37.55)	2.9	NA	
Minishear Coupon	4,989 (34.40)	2.2	111,731 (770.36)	7.4

Conclusions

Interlayer weld strength was successfully investigated using in-plane shear testing. For these high weld strength coupons, the ASTM D3846 notched coupon test suffered from excessive gage section rotation, which caused interference with the test fixture. However, a new test method using minishear coupons provided repeatable results for both strength and modulus, which compared quite well with bulk properties. Two new test methods were developed to directly measure shear and tensile properties of the polymer filament. Oven treatment of filament above T_g was shown to reduce the effect of preferential molecular alignment caused by extrusion manufacture of the filament, and oven-treated filament properties are considered to provide a good representation of bulk properties. All three new test methods provided good to very good repeatability across a large number of replicates.

Acknowledgments

The authors would like to acknowledge their respective organizations for supporting the work presented here. Within AON3D, the hard work of Alfredo Constantini in manufacturing the AON3D ABS Prime coupon blocks is recognized. Within NRC, the hard work of Richard Desnoyers and Dmitrii Klishch is acknowledged in supporting the specimen testing despite the ongoing pandemic. Within Ryerson University, Seyed Miri deserves recognition for design and 3D printing of the grips for filament tensile testing.

References

1. D. Popescu, A. Zapciu, C. Amza, F. Baciu, and R. Marinescu, "FDM Process Parameters Influence Over the Mechanical Properties of Polymer Specimens: A Review," *Polymer Testing* 69 (2018): 157–166, https://doi.org/10.1016/j.polymertesting.2018.05.020

2. K. Fayazbakhsh, M. Movahedi, and J. Kalman, "The Impact of Defects on Tensile Properties of 3D Printed Parts Manufactured by Fused Filament Fabrication," *Materials Today Communications* 18 (2019): 140–148, https://doi.org/10.1016/j.mtcomm.2018.12.003

3. S. Guessasma, S. Belhabib, and H. Nouri, "Microstructure and Mechanical Performance of 3D Printed Wood-PLA/PHA Using Fused Deposition Modelling: Effect of Printing Temperature," *Polymers* 11, no. 11 (2019), https://doi.org/10.3390/polym11111778

4. M. Faes, E. Ferraris, D. and Moens, "Influence of Inter-Layer Cooling Time on the Quasi-Static Properties of ABS Components Produced via Fused Deposition Modelling," *Procedia CIRP* 42 (2016): 748–753, https://doi.org/10.1016/j.procir.2016.02.313

5. W. Lin, H. Shen, G. Xu, L, Zhang, J. Fu, and X. Deng, "Single-Layer Temperature-Adjusting Transition Method to Improve the Bond Strength of 3D-Printed PCL/PLA Parts," *Composites Part A: Applied Science and Manufacturing* 115 (2018): 22–30, https://doi.org/10.1016/j.compositesa.2018.09.008

6. V. Kuznetsov, A. Tavitov, O. Urzhumtsev, M. Mikhalin, and A. Moiseev, "Hardware Factors Influencing Strength of Parts Obtained by Fused Filament Fabrication," *Polymers* 11, no. 11 (2019), https://doi.org/10.3390/polym11111870

7. W. Ferrell, C. Arndt, and S. TerMaath, "Tensile Strength Dependence of FFF Fiber Reinforced ABS on Environmental Conditioning," *Mechanics of Advanced Materials and Structures* (2020): 1–14, https://doi.org/10.1080/15376494.2020.1722870

8. *Standard Test Method for In-Plane Shear Strength of Reinforced Plastics*, ASTM D3846-08(2015) (West Conshohocken, PA: ASTM International, approved Sept. 1, 2015), https://doi.org/10.1520/D3846-08R15

9. Z. Weng, J. Wang, T. Senthil, and L. Wu, "Mechanical and Thermal Properties of ABS/Montmorillonite Nanocomposites for Fused Deposition Modeling 3D Printing," *Materials & Design* 102 (2016): 276–283, http://dx.doi.org/10.1016/j.matdes.2016.04.045

10. A. Rahimizadeh, J. Kalman, K. Fayazbakhsh, and L. Lessard, "Recycling of Fiberglass Wind

Turbine Blades into Reinforced Filaments for Use in Additive Manufacturing," *Composites Part B: Engineering* 175 (2019), https://doi.org/10.1016/j.compositesb.2019.107101

11. R. Cole, A. Avalos, and A. Walker, "Effect of Process Parameters on Mechanical Properties of 3D Printed Carbon-Fibre PEEK," in *Proceedings of Fourth International Symposium on Automated Composites Manufacturing: ACM4*, ed. S. V. Hoa (Lancaster, PA: DEStech Publications, 2019), TK–TK.

12. *Standard Terminology for Additive Manufacturing—Coordinate Systems and Test Methodologies*, ASTM ISO/ASTM 52921-13(2019) (West Conshohocken, PA: ASTM International, approved April 1, 2019), https://doi.org/10.1520/ISOASTM52921-13R19

13. J. Rodriguez, J. Thomas, and J. Renaud, "Mechanical Behavior of Acrylonitrile Butadiene Styrene (ABS) Fused Deposition Materials—Experimental Investigation," *Rapid Prototyping Journal* 7, no. 3 (2001): 148–158, https://doi.org/10.1108/13552540110395547

14. *Standard Test Method for Shear Testing of Aluminum and Aluminum-Alloy Rivets and Cold-Heading Wire and Rods*, ASTM B565-04(2015) (West Conshohocken, PA: ASTM International, approved October 1, 2015), https://doi.org/10.1520/B0565-04R15